Progress In Electromagnetics Research Letters, Vol. 3, 161–168, 2008

TIME DOMAIN CHARACTERISTICS OF A DOUBLE-PRINTED UWB DIPOLE ANTENNA

F.-J. Wang and J.-S. Zhang

School of Information Science & Engineering
Lanzhou University
Room 404, XinXi Lou, 222# Tian Shui Road, Lanzhou 730000, China

X.-X. Yang

School of Communication and Information Engineering
Shanghai University
Shanghai 200072, China

G.-P. Gao

School of Information Science & Engineering
Lanzhou University
Room 404, XinXi Lou, 222# Tian Shui Road, Lanzhou 730000, China

1. INTRODUCTION

With the development of UWB communications, UWB antennas for wireless applications have received much attention. Various antennas have been proposed for UWB application [1–8]. Antenna design is a particular challenge in UWB systems. Due to the extremely wide operating bandwidth, the UWB antennas impose significant impacts on the received waveforms. Thus, a good time domain performance is a primary requirement of a suitable UWB antenna. Besides, a good design of UWB antenna should be optimal for the performance of overall systems.

Planar dipole antennas are suitable for wide band applications due to their broad impedance bandwidths and compact size [9]. Recently, some planar dipole antennas have been proposed for UWB applications. For example, the double printed circular disk antenna, offset-fed square dipole, stepped-fat dipole, and diamond dipole were studied for UWB systems [10–13]. Those antennas show good

impedance characteristics and a little higher gains over 3.1 GHz to 10.6 GHz UWB band.

In this paper, on the basis of our former study, the time domain performances of a double-printed UWB dipole antenna are investigated for both single band and multi-band schemer. An antenna system composed of double printed UWB dipole antennas was fabricated and measured in frequency domain. With the aid of inverse Fourier fast transforms, impulse responses in time domain were obtained and studied.

2. ANTENNA STRUCTURE AND ANTENNA SYSTEM

The structure of the double-printed UWB dipole antenna is shown in Fig. 1. The antenna is printed on both sides of a substrate with $\varepsilon_r = 2.78$ and a thickness of 0.8 mm. The total size of the antenna is $46 \times 48\,\text{mm}^2$. The dark parts are on the front plane of the substrate while the light parts are on the back plane. The dipole is composed of two rectangular arms and is fed by parallel plate and microstrip line. The different widths of the fed line improved the impedance matching. The measured and simulated voltage standing wave ratios (VSWR) are shown in Fig. 2. The simulation was carried out by using an EM software based on the method of finite integration technology. It can be observed that both the simulated and measured results cover the UWB band from 3.1 GHz–10.6 GHz with VSWR less than 2. The measured result is a little wider than the simulated result. This is mainly due to the measurement error and numerical error.

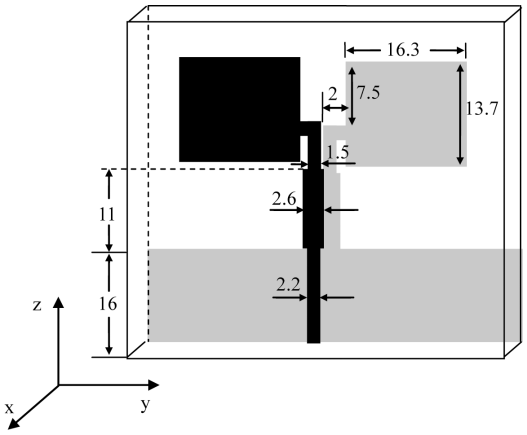

Figure 1. The structure of double-printed UWB dipole antenna.

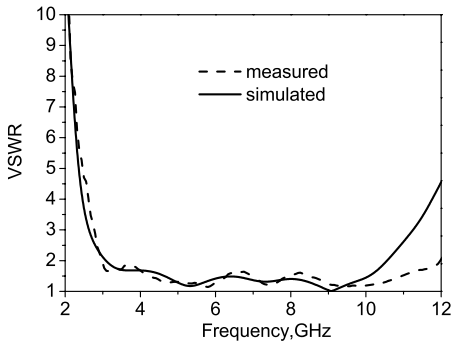

Figure 2. The measured and simulated VSWR.

In order to evaluate the antenna performance from a system point of view, a transmitting/receiving antenna system composed of two double-printed UWB dipole antennas was fabricated and tested by using vector network analyzer (VNA) HP8720ES. The transmitting and receiving antennas are positioned in two scenarios, i.e., face to face and end to end, with a distance of 0.5 m as plotted in Fig. 3.

Figure 3. Measured scenarios. (a) End to end. (b) Face to face.

The system transfer functions S_{21} for the two scenarios are shown in Fig. 4 and Fig. 5 respectively. It should be noted that the measurement was carried out in an indoor environment with reflecting objects in the surrounding area. Satisfactory agreement between simulation and measurement results is observed. In the UWB band, the behaviors of transfer functions are acceptable for the two scenarios. The amplitudes are relative flat and the phases are nearly linear.

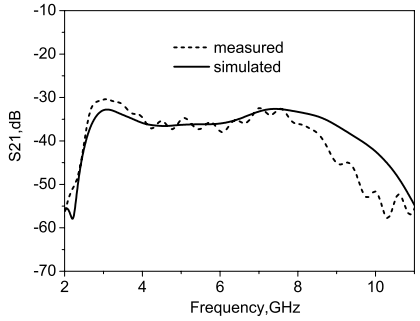

Figure 4. Amplitude of the system transfer functions: End to end.

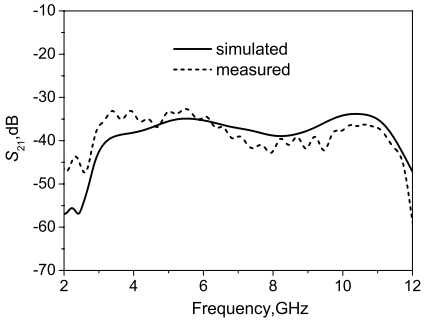

Figure 5. Amplitude of the system transfer functions: Face to face.

3. TIME DOMAIN PERFORMANCE

3.1. Performance in a Single Band Scheme

In a single band scheme, each transmitted pulse may occupy the entire UWB band. The fifth order Rayleigh pulse with $\sigma = 75\,\text{ps}$ is used as the voltage source in this paper, which meets the FCC spectral mask requirement for indoor systems [14].

Figure 6 shows the simulated radiated pulse waveforms in different directions. The curves have already been normalized to their respective maximum values. Nearly the same radiated waveforms can be observed in different five directions of x-z plane. So the characteristics of the double printed UWB dipole are very stable with the radiation angles. It also can be observed that the radiated pulses waveforms are little distorted as compared to the source pulse.

The spectral of the received signals at the receiving antenna can be calculated using the following formula:

$$V_r(\omega) = V_t(\omega) \cdot S_{21}(\omega) \tag{1}$$

Then the time domain pulse can be obtained by using inverse Fourier transform. The received pulse waveforms of the two scenarios are plotted in Fig. 7. The two received pulses matches with each other very well. The late time ringing is almost negligible. The received pulses are a little distorted due to the variations of the system transfer functions. The received waveforms are similar to higher order differentiated Rayleigh pulses, which reflects the differentiator property of the antenna.

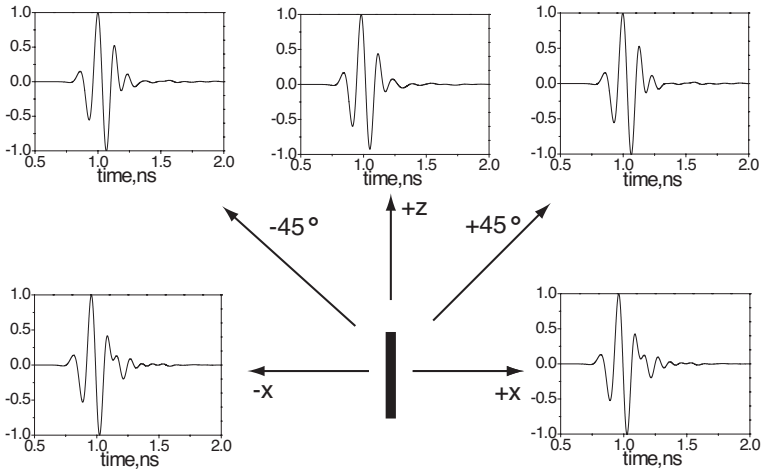

Figure 6. Radiated pulses in x-z plane with different angles.

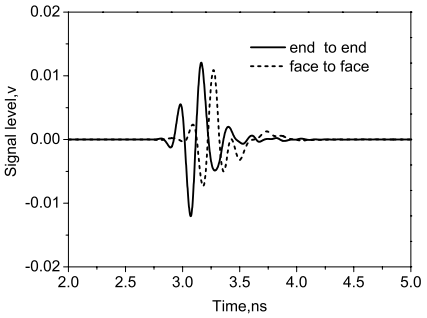

Figure 7. Received pulses for single band schemer.

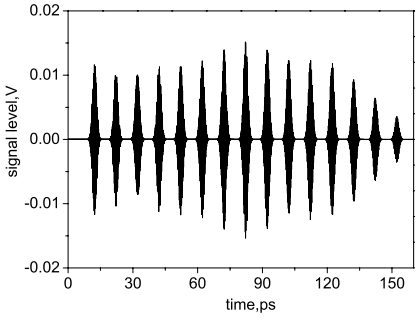

Figure 8. Received pulses of end to end scenario for multiband schemer.

3.2. Multiband Scheme

In the multiband schemer, the available UWB band is divided into 15 sub-bands [14]. Each sub-band has a 10 dB bandwidth of 500 MHz. The input voltage at the transmitting antenna is a series of modulated Gaussian pulses, each having a 10 dB bandwidth of 500 MHz but different central frequencies, as defined in (2). The parameter $\sigma =$ 1336 ps. The carrier frequency increases from 3.35 GHz for the first pulse to 10.35 GHz for the last pulse. So the spectral of the v_t covers

the entire UWB band.

$$v_t = \sum_{n=0}^{14} \sin\left[\left(2\pi\left(3.35\times10^9 + n\times0.5\times10^9\right)\right)t\right] \times \exp\left[-\left(\frac{t-(n+1)\times10}{\sigma}\right)^2\right] \quad (2)$$

The received waveforms in multiband scheme are shown in Fig. 8 and Fig. 9 for end to end and face to face scenarios respectively. It is clearly observed that the amplitude of S_{21} obviously affects the amplitudes of received pulses in different sub-bands. The envelopes of the received pulses correspond well to the shapes of S_{21}. With flat amplitude of S_{21}, the received signals in all the subbands can be detected well. In contrast, the uneven S_{21} will lead to unequal amplitude of received pulses, thus results in different signal to noise ratio in the sub-bands.

The envelope of the received pulses of end to end scenario is flatter than that of the face to face scenario. The last received pulse of the end to end scenario is lower than others because of the decrease of the S_{21} after 10 GHz. The received pulses are little distorted and the ringing is negligible.

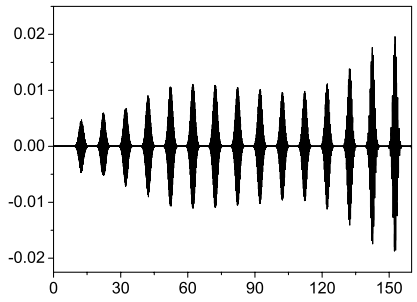

Figure 9. Received pulses of face to face scenario for multiband schemer.

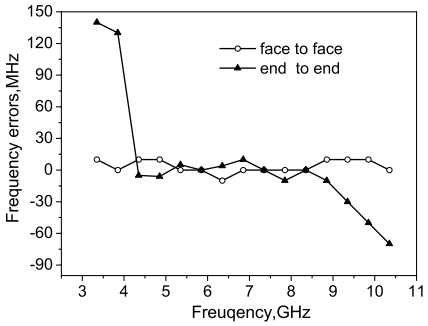

Figure 10. Frequency errors for multiband schemer.

Study has shown that the uneven amplitude of S_{21} also introduces frequency errors defined as the differences of central frequency between the received pulses and the source pulses [11]. Fig. 10 demonstrates the frequency errors in multiband schemer of the two scenarios. It can be observed that the frequency errors are less than 10 MHz for face to face scenario while the maximum frequency error for end to

end scenario is nearly 140 MHz. The curves of frequency errors are closed related to the amplitude of S_{21} displayed in Fig. 8 and Fig. 9. A monotonically increasing S_{21} in the band of a source pulse increases the central frequency of the signal, thus introducing a positive frequency error, and vice versa [11]. This can also be observed from Fig. 8–Fig. 10.

4. CONCLUSION

Based on the frequency domain results, the time domain characteristics of the double printed UWB antenna have been investigated for both single band and multi-band schemer. For single band schemer, the radiated pulse waveforms are little distorted in the H plane and the received pulses matching well to each other with no obvious ringing. For multiband schemer, almost similar amplitude responses of the received pulses in different sub-bands are obtained when the transmitting and receiving antennas are located end to end. The frequency errors are less than 10 MHz for face to face scenario. Measurement and simulated results have shown that the double printed UWB antenna can operate over the FCC defined UWB band.

REFERENCES

1. Khan, S. N., J. Hu, J. Xiong, and S. He, "Circular fractal monopole antenna for low vswr UWB applications," *Progress In Electromagnetics Research Letters*, Vol. 1, 19–25, 2008.
2. Yin, X.-C., C. Ruan, C. Y. Ding, and J.-H. Chu, "A planar U type monopole antenna for UWB applications," *Progress In Electromagnetics Research Letters*, Vol. 2, 1–10, 2008.
3. Naghshvarian-Jahromi, M., "Compact UWB bandnotch antenna with transmission-line-fed," *Progress In Electromagnetics Research B*, Vol. 3, 283–293, 2008.
4. Sadat, S., M. Fardis, F. G. Kharakhili, and G. Dadashzadeh, "A compact microstrip square-ring slot antenna for UWB applications," *Progress In Electromagnetics Research*, PIER 67, 173–179, 2007.
5. Sadat, S., M. Houshmand, and M. Roshandel, "Design of a microstrip square-ring slot antenna filled by an H-shape slot for UWB applications," *Progress In Electromagnetics Research*, PIER 70, 191–198, 2007.
6. Zaker, R., C. Ghobadi, and J. Nourinia, "A modified microstrip-fed two-step tapered monopole antenna for UWB and wlan

applications," *Progress In Electromagnetics Research*, PIER 77, 137–148, 2007.

7. Ren, W., Z. G. Shi, and K. S. Chen, "Novel planar monopole UWB antenna with 5-GHz band-notched characteristic," *Journal of Electromagnetic Waves and Applications*, Vol. 21, No. 12, 1645–1652, Oct. 2007.
8. Gopikrishna, M., D. D. Krishna, A. R. Chandran, and C. K. Aanandan, "Square monopole antenna for ultra wide band communication applications," *Journal of Electromagnetic Waves and Applications*, Vol. 21, No. 11, 1525–1537, Sept. 2007.
9. Wang, F. J. and J. S. Zhang, "Wideband printed dipole antenna for multiple wireless services," *Journal of Electromagnetic Waves and Applications*, Vol. 21, No. 11, 1469–1477, Sep. 2007.
10. Sheng, J., X. X. Yang, J. T. Sun, and Y. M. Lu, "Double-printed circular disc antenna having a frequency band notch function," *Microwave and Optical Technology Letters*, Vol. 49, No. 11, 2675–2677, Aug. 2007.
11. Wu, X. H., Z. N. Chen, and N. Yang, "Optimization of planar diamond antenna for single-band and multiband uwb wireless communications," *Microwave and Optical Technology Letters*, Vol. 42, No. 6, 451–455, Sep. 2004.
12. Young, J. P. and J. H. Song, "Development of ultra wideband planar stepped-fat dipole antenna," *Microwave and Optical Technology Letters*, Vol. 48, No. 9, Sep. 2006.
13. Wu, X. H. and Z. N. Chen, "Comparison of planar dipoles in UWB applications," *IEEE Trans. Antennas Propag.*, Vol. 53, No. 6, 1973–1981, June 2005.
14. Chen, Z. N. and X. H. Wu, "Consideration for source pulse and antennas in UWB radio system," *IEEE Transactions on Antennas and Propagation*, Vol. 52, No. 7, 1739–1748, July 2004.